# Amphiphysin Heterodimers: Potential Role in Clathrin-mediated Endocytosis

**Patrick Wigge, Katinka Köhler, Yvonne Vallis, Christopher A. Doyle, David Owen, Stephen P. Hunt, and Harvey T. McMahon***

The Neurobiology Division, Medical Research Council Laboratory of Molecular Biology, Cambridge, CB2 2QH, United Kingdom

Amphiphysin (Amph) is a src homology 3 domain-containing protein that has been implicated in synaptic vesicle endocytosis as a result of its interaction with dynamin. In a screen for novel members of the amphiphysin family, we identified Amph2, an isoform 49% identical to the previously characterized Amph1 protein. The subcellular distribution of this isoform parallels Amph1, both being enriched in nerve terminals. Like Amph1, a role in endocytosis at the nerve terminal is supported by the rapid dephosphorylation of Amph2 on depolarization. Importantly, the two isoforms can be coimmunoprecipitated from the brain as an equimolar complex, suggesting that the two isoforms act in concert. As determined by cross-linking of brain extracts, the Amph1–Amph2 complex is a 220- to 250-kDa heterodimer. COS cells transfected with either Amph1 or Amph2 show greatly reduced transferrin uptake, but coexpression of the two proteins rescues this defect, supporting a role for the heterodimer in clathrin-mediated endocytosis. Although the src homology 3 domains of both isoforms interact with dynamin, the heterodimer can associate with multiple dynamin molecules in vitro and activates dynamin's GTPase activity. We propose that it is an amphiphysin heterodimer that drives the recruitment of dynamin to clathrin-coated pits in endocytosing nerve terminals.

## INTRODUCTION

All clathrin-mediated endocytosis, including synaptic vesicle recycling, requires dynamin (De Camilli *et al.*, 1995). Originally identified in *Drosophila* (Poodry and Edgar, 1979), this large GTP-binding protein appears to act by pinching off vesicles at constricted clathrin-coated pits. Many experiments (Herskovits *et al.*, 1993; van der Bliek *et al.*, 1993; Damke *et al.*, 1994; Hinshaw and Schmid, 1995; Takei *et al.*, 1995) suggest that it does so by forming an oligomeric ring at the collar of the vesicle that, through a conformational change likely effected by GTP hydrolysis, is thought to drive

vesicle fission. The brain protein amphiphysin (Amph)[1] has recently emerged as a likely candidate for a dynamin-binding protein (David *et al.*, 1996). Amph was originally identified as a synaptic-vesicle–associated protein (Lichte *et al.*, 1992). In addition to its interaction with dynamin, it has been reported to interact via a distinct domain with the α subunit of the adaptor protein complex 2 (AP-2) adaptor complex (Wang *et al.*, 1995; David *et al.*, 1996). In vitro, amphiphysin can interact with both α-adaptin and dynamin simultaneously (Wigge *et al.*, 1997). Thus, the original proposal (David *et al.*, 1996) that amphiphysin could potentially recruit dynamin to clathrin-coated pits, perhaps via its interaction with plasma membrane adaptors, has some experimental support.

Several lines of evidence corroborate these in vitro studies by showing that Amph may have a crucial role in endocytosis in vivo. Firstly, it has been shown that disruption of dynamin–Amph interactions by recombinant Amph src homology 3 (SH3) domain in vivo

---

* Corresponding author.

[1] Abbreviations used: Amph, amphiphysin; AP-2, adaptor protein complex 2; BIN1, box-interacting protein 1; DTSSP, 3,3'-dithiobis(sulfosuccinimidylpropionate); EST, express sequence tag; GST, glutathione *S*-transferase; PCR, polymerase chain reaction; PKC, protein kinase C; PMA, phorbol 12-myristate 13-acetate; Rvs, reduced viability upon nutrient starvation; SH3, src homology 3.

leads to a potent block in clathrin-mediated endocytosis (Shupliakov *et al.*, 1997; Wigge *et al.*, 1997). Secondly, in the rare autoimmune disease stiff-man syndrome, antibodies are sometimes made to the SH3 domain of Amph (David *et al.*, 1994); these autoantibodies are implicated in causing the neurological defects apparent in these patients. Finally, there are two proteins in yeast, rvs161 and rvs167 (where rvs is reduced viability upon nutrient starvation), that are weakly homologous to Amph, and mutations in either of these proteins cause a reduction in endocytosis (Munn *et al.*, 1995).

Although there is clearly some evidence for a putative role of Amph in clathrin-mediated uptake processes, the precise mechanism by which Amph acts remains unclear. To further unravel the proteins involved in endocytosis, we have searched for other Amph family members. In this article, we demonstrate the presence of an Amph heterodimer in rat brain, consisting of the previously cloned Amph1 and a shorter isoform, which we call Amph2. The heterodimer has the capacity to interact with multiple dynamin molecules through its two SH3 domains and activate dynamin's GTPase in vitro. In COS-7 cells, overexpression of either Amph1 or Amph2 alone potently blocks transferrin uptake, but if the two are expressed together, endocytosis is rescued, further supporting the hypothesis that the Amph heterodimer is the functional unit in endocytosis. We speculate that the heterodimer is the main factor driving the recruitment of dynamin to clathrin-coated pits, its enrichment in the brain perhaps helping to explain the speed of the specialized pathway of synaptic vesicle recycling.

## MATERIALS AND METHODS

### Cloning of Amph1 and Amph2

Amph1 was cloned from a Matchmaker rat brain cDNA library (Clontech, Palo Alto, CA) by using degenerate primers (atggccgacatsaagacgggcatcttcgcc and ctawtcyarrtgkcgkgtgaagttctctgg) from comparison of the chick and human sequences. By comparison of human expressed sequence tags with the human Amph1 gene, we noted the presence of another human isoform. By using degenerate oligonucleotides (atggcngaratgggnwsnaarggngtnacngcrggnaa and yyanggnacnckytcngtraarttytcnggraanacnccnc), we generated a probe by PCR to screen a rat brain cortex cDNA library, in the lambda ZAP II vector (Stratagene, La Jolla, CA). Twenty positive clones were analyzed that extensively overlapped. Six of the clones encoded a longer version of the protein with an insert of 108 nucleotides. The complete cDNA was entirely sequenced from several overlapping clones by using Dye terminator cycle sequencing on a Perkin Elmer-Cetus Applied Biosystems model 377 sequencer with Amplitaq FS.

The Amph2 splice variants Amph2–1 (seven clones), Amph2–2 (five clones), and Amph2–4 (one clone) were found while screening the brain cDNA library for Amph1 isoforms. Amph2–3 and Amph2–5 were identified by polymerase chain reaction (PCR) amplification from the same library, and Amph2–6 was obtained three times from a kidney library. The partial clone of rat Amph2–7 we

have identified corresponds to the human box-interacting protein 1 (BIN1) isolated by Sakamuro *et al.* (1996).

### Plasmid Construction

The vectors pGEX-4T2 (Pharmacia, Piscataway, NJ) and pET-15b (Novagen) were used to make fusion proteins with glutathione *S*-transferase (GST) and hexahistidine tags, respectively. The following constructs, cloned by PCR, were used: GST-, His-, and pCMV-Amph1, full-length rat Amph1 in pGEX-4T2, pET-15b, and pCMV5, respectively; GST-Amph1-SH3, residues 596–683; GST- and pCMV-Amph2–1, full-length rat Amph2–1; GST-Amph2-SH3, residues 494–588.

### Immunocytochemistry

Three adult male Sprague–Dawley rats, deeply anesthetized with saturated chloral hydrate (1 ml, intraperitoneally), were transcardially perfused with fixative (4% paraformaldehyde in 0.1 M phosphate buffer, pH 7.2). The brains were removed, postfixed for 6 h, and cryopreserved (48 h) in 30% sucrose with phosphate buffer. Frozen sagittal sections (40 $\mu$m) of brain were incubated for 48 h in Amph2 antiserum (1:1000 dilution, 4°C; tested for cross-reactivity in Figure 2) and the presence of this protein was visualized with avidin-biotin-fluorescein isothiocyanate immunofluorescence. Control sections for the immunohistochemistry were prepared by omitting the primary antiserum from the incubation medium or by preadsorption with the native protein (10 $\mu$g/ml) and show no immunoreactivity. Sections were mounted under coverslips and viewed with conventional epifluorescence or with a Bio-Rad MRC-600 confocal microscope for specific immunostaining of Amph2.

### Electron Microscopy

Two rats were transcardially perfused with 4% paraformaldehyde, 0.1% glutaraldehyde, and 15% saturated picric acid in 0.1 M phosphate buffer, pH 7.4, for 5 min. Vibratome sections (40 $\mu$m) of the cerebellum were cut and processed for Amph2 immunostaining as described above. After the 3,3'-diaminobenzidine reaction, sections containing specific Amph2 staining were postfixed in 1% osmium tetroxide for 1 h and dehydrated through a series of ethanol solutions. "En bloc" staining was performed with a 1% solution of uranyl acetate in 70% ethanol. After dehydration, the sections were cleared in propylene oxide (two 10-min rinses) and placed in fresh Durcurpan (Fluka Chemical, Buchs, Switzerland) overnight. They were then flat-embedded in Durcurpan between cellulose acetate foils and polymerized at 60°C for 48 h. When polymerization was complete the sections were attached to Durcurpan blocks and ultrathin (pale gold interference fringe; 70–90 nm) sections were cut with a diamond knife (Diatome, Fort Washington, PA) on a ultramicrotome. Sections were stained with Reynold's lead citrate for 2 to 3 min and examined with the electron microscope. This technique baises toward membrane labeling due to either cross-linking of proteins to membranes during fixation or the diffusion of the 3,3'-diaminobenzidine label, thus a cytosolic pool of Amph is not clearly seen.

### Tissue Fractionations

Total brain homogenate was prepared from frozen rat brains homogenized in buffer A [150 mM NaCl, 20 mM HEPES, pH 7.4, 1 mM MgCl$_2$, 1 mM EGTA, and a protease inhibitor mixture (10 $\mu$g/ml leupeptin, 100 $\mu$g/ml Pefabloc, 10 $\mu$g/ml aprotinin, and 1 $\mu$g/ml pepstatin)], followed by solubilization with 1% Triton X-100. Debris was pelleted at 100,000 $\times$ *g* for 10 min, and the supernatant was used for experiments at approximately 5–10 mg/ml. Other tissue homogenates were prepared in a similar manner.

Subcellular fractionation of rat brain was carried out essentially according to McMahon *et al.* (1992). Synaptosomes were prepared in HBM (HEPES-buffered medium: 140 mM NaCl, 5 mM KCl, 20 mM

HEPES, pH 7.4, 5 mM NaHCO$_3$, 1 mM MgCl$_2$, 1.2 mM Na$_2$HPO$_4$, 10 mM glucose) and their integrity was checked before experiments by monitoring glutamate exocytosis with a fluorometric assay as described in McMahon and Nicholls (1991). Synaptic vesicles were purified as described in Fykse *et al.* (1993).

### Binding Studies

GST fusion proteins and His$_6$-tagged fusion proteins were expressed in *Escherichia coli* and purified on glutathione-agarose and nickel-nitrilotriacetic acid (Ni-NTA)-agarose resins, respectively. Purified protein attached to beads was incubated with either total rat brain homogenate or with COS cell expressed proteins (essentially as described in McMahon and Südhof, 1995). Immunoprecipitations were carried out with 10 $\mu$g of antibody per 5 mg of brain extract, plus 10 $\mu$l of protein A/G-Sepharose. After 2 h of gentle mixing, the beads were pelleted at 5000 $\times$ *g* for 2 min and washed three times in the same buffer. Bound protein was eluted by boiling in an equal volume of 2$\times$ sample buffer and separated by SDS-PAGE (7 or 13% gels) for immunoblotting (using National Diagnostics reagents, Atlanta, GA) and or Coomassie staining.

### Phosphorylation Studies

Phosphorylation of synaptosome proteins was carried out by incubating synaptosomes (1 mg/ml) with [$^{32}$P]orthophosphate (1 mCi/ml) in HBM containing 10 mM glucose and 0.1 mM CaCl$_2$ for 1 h. Synaptosomes were resuspended in fresh HBM and stimulated with 35 mM KCl for 1 min at 37°C in the presence or absence of 1 mM calcium. After rapid freezing in liquid nitrogen, the synaptosomes were thawed and lysis was completed with 1% Triton X-100, 2.5 mM EGTA, 1 mM dithiothreitol, and the protease inhibitor mixture. Cleared lysate was then used for immunoprecipitations, followed by SDS-PAGE and transfer onto nitrocellulose. Radioactivity was quantitated by PhosphorImager analysis.

### GTPase Experiments

Purified dynamin (0.5 $\mu$g) was incubated in 50 $\mu$l of 20 mM HEPES, pH 7.4, 20 mM NaCl, 1 mM dithiothreitol, 100 $\mu$M GTP, 0.1 $\mu$M [$\alpha$-$^{32}$P]GTP, at 37°C for 20 min in the presence of 2 $\mu$g of each effector. The Amph heterodimer was purified by Amph2 immunoprecipitation from brain extract. Grb2 or isolated SH3 domains were expressed in bacteria. Reactions were terminated by heating to 65°C for 10 min and separated on polyethyleneimine-cellulose by thin layer chormatography, followed by autoradiography.

### Transferrin Uptake Assay

COS 7 cells were transiently transfected as described by Wigge *et al.* (1997) with pCMV-Amph1 and pCMV-Myc-Amph2. After 36 h cells were incubated in serum-free DMEM for 1 h and then with DMEM containing 25 $\mu$g/ml biotinylated transferrin (Sigma, St. Louis, MO). Amph 1 was visualized after paraformaldehyde fixation with anti-Amph1 followed by Texas Red anti-rabbit secondary antibody (Vector Laboratories, Burlingame, CA). Amph2 was detected with 9E10 anti-MYC antibody followed by Cy5-conjugated goat anti-mouse antibody. Transferrin was visualized with fluorescein isothiocyanate-avidin.

### Antibodies

Antibodies against Amph1 and Amph2 were raised by injecting the N terminus of Amph1 and His-Amph2–1 proteins, respectively, into rabbits (three 100-$\mu$g injections). Other antibodies used were against Dynamin (D632, Tom Südhof, HHMI, UT Southwestern Medical Center, Dallas), synaptobrevin (Cl69.1, Reinhard Jahn, HHMI, Yale University), synaptotagmin (V216, Tom Südhof), $\alpha$-adaptin (AC1-M11 from Margaret Robinson, Cambridge University, England),

$\gamma$-adaptin (Transduction Laboratories, Lexington, KY), and MYC (9E10, Sean Munro, MRC, Cambridge, England).

## RESULTS

### Cloning of Amph2

From comparison of the human Amph1 sequence with expressed sequence tags from the database, we designed degenerate primers that were used to make probes by PCR to screen a rat brain cortex cDNA library. Sequencing revealed the rat homologue of the previously cloned 125-kDa Amph protein (which we call Amph1). In addition, a second smaller cDNA was sequenced, encoding a protein of 588 amino acids. We named this protein Amph2 because it has 49% amino acid identity to Amph1 (Figure 1A). Amph1 and Amph2 are highly conserved at their N and C termini (Figure 1B), indicating a likely conservation of function, but there is also a region largely unique to Amph1 (Domain III). Like Amph1, the C-terminal region of Amph2 (Domain IV) is predicted to be an SH3 domain. It contains two critical residues (Gly and Pro, marked with asterisks in Figure 1A) that, when mutated in the *SEM-5* SH3 domain, result in a nonfunctional protein (Clark *et al.*, 1992), and are conserved in Amph1 and Amph2 alignments. Amph2 has no predicted transmembrane domains.

The predominant forms of Amph2 in the cDNA library were Amph2–1 and Amph2–2 (see MATERIALS AND METHODS). However, we identified many other splice variants of Amph2, some from the cDNA library and at least 10 bands (our unpublished results) can be identified from rat brain cDNA by PCR out of the conserved domains at the N and C termini. Figure 1C shows where the splicing occurs in the sequenced clones, including the recently published BIN1 protein (Sakamuro *et al.*, 1996) for which we have a partial clone.
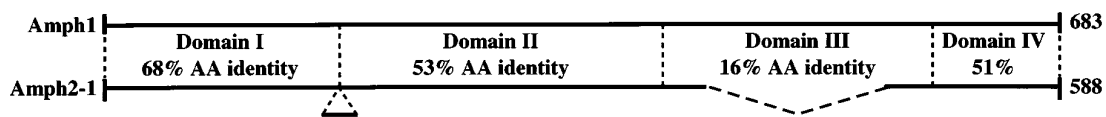
### Amph2 Is a 92-kDa Protein That Has a Tissue and Subcellular Distribution Closely Paralleling Amph1

A polyclonal antibody to Amph2 was generated by using bacterially expressed Amph2–1 protein. As shown in Figure 2A, this antibody reacts predominantly with a 92-kDa band in brain (a weaker band just below Amph2–1 is probably due to the slightly smaller Amph2–2 protein, which was found by cDNA screening to be the next most common splice variant in the brain). Amph2–1 expressed in COS cells comigrates with the 92-kDa band in brain, with an additional band sometimes seen at 95 kDa (likely a posttranslational modification). The anomalous behavior on PAGE (predicted molecular mass of 65 kDa) is due to a region of the protein that is spliced out in Amph2–5 (our unpublished results); Amph1 similarly migrates slower on gels than predicted (Lichte *et al.*,

**A**

| | | |
|---|---|---|
| cAmph | MADMKT GIFAKNVQKRLNRAQEKVLQKLGKADETKDEQFEEYVQNFKRQEAEGSRLQRELRAYLAAIKGMQDASK | 75 |
| hAmph | MADIKT GIFAKNVQKRLNRAQEKVLQKLGKADETKDEQFEEYVQNFKRQEAEGTRLQRELRGYLAAIKGMQEASM | 75 |
| Rat Amph1 | MADIKT GIFAKNVQKRLNRAQEKVLQKLGKADETKDEQFEEYVQNFKRQEAEGTRLQRELRGYLAAIKGMQEASM | 75 |
| Rat Amph2 | MAEMGSKGVTAGKIASNVQKKLTRAQEKVLQKLGKADETKDEQFEQVQNFNKQLTEGTRLQKDLRTYLASVKAMHEASK | 80 |

| | | |
|---|---|---|
| cAmph | KLTESLHEVYEPDWYGREDVKMIGEKCDELWEDFHQKLVDGSLLTLDTYLGQFPDIKTRIAKRSRKLVDYDSARHHLEAL | 155 |
| hAmph | KLTESLHEVYEPDWYGREDVKMVGEKCDVLWEDFHQKLVDGSLLTLDTYLGQFPDIKNRIAKRSRKLVDYDSARHHLEAL | 155 |
| Rat Amph1 | KLTESLHEVYEPDWYGREDVKMVGEKCDVLWEDFHQKLVDGSLLTLDTYLGQFPDIKNRIAKRSRKLVDYDSARHHLEAL | 155 |
| Rat Amph2 | KLSECLQEVYEPEWPGRDEANKIAENNDLLWMDYHQKLVDQALLTMDTYLGQFPDIKSRIAKRGRKLVDYDSARHHYESL | 160 |

| | | |
|---|---|---|
| cAmph | QSSKRKDEGRIIK AEEEFQKAQKVFEEFNTDLQEELPSLWSRRVGFYVN | 204 |
| hAmph | QSSKRKDESRISK AEEEFQKAQKVFEEFNVDLQEELPSLWSRRVGFYVN | 204 |
| Rat Amph1 | QSSKRKDESRISK AEEEFQKAQKVFEEFNVDLQEELPSLWSRRVGFYVN | 204 |
| Rat Amph2 | QTAKKKDEAKIAKPVSLLEKAAPQWCQGKLQAHLVAQTNLLRNQAEEELIKAQKVFEEMNVDLQEELPSLWNSRVGFYVN | 240 |

| | | |
|---|---|---|
| cAmph | TFKNVSSLEAKFHKEIALLCHKLYEVMTKLGDQHADKAFTIQGAPSDSGPLRIAKTPSPPEEVSPLPSPTASPNHMLAPA | 284 |
| hAmph | TFKNVSSLEAKFHKEIAVLCHKLYEVMTKLGDQHADKAFTIQGAPSDSGPLRIAKTPSPPEEPSPLPSPTASPNHTLAPA | 284 |
| Rat Amph1 | TFKNVSSLEAKFHKEIAVLCHKLYEVMTKLGDQHADKAFSIQGAPSDSGPLRIAKTPSPPEEASPLPSPTASPNHTLAPA | 284 |
| Rat Amph2 | TFQSIAGLEENFHKEMSKLNQNLNDVLVSLEKQHGSNTFTVKAQPSDSAPEKGNKSPSPPPDGSPAATPEIRVNHEPEPA | 320 |

| | | |
|---|---|---|
| cAmph | S PAPARPKSPTQLRKGPPVPPLPKLTPTKELQQENIINLFDDNFVPEINVTTPSQNEIPETK KVESLLDLDFDPFK | 360 |
| hAmph | S PAPARPRSPSQTRKGPPVPPLPKVTPTKELQQENIISFFEDNFVPEISVTTPSQNEVPEVK KEETLLDLDFDPFK | 360 |
| Rat Amph1 | S PAPVRPRSPSQTRKGPPVPPLPKVTPTKELQQENIINFFEDNFVPEINVTTPSQNEVLLEVK KEETLLDLDFDPFK | 360 |
| Rat Amph2 | SGASPGATIPKSPSQLRKGPPVPPPPKHTPSKEMKQEQILSLFDDAFVPEISVTTPSQFEAPGPFSEQASLLDLDFELPLP | 400 |

| | | |
|---|---|---|
| cAmph | PEVV STGVTHSPMSQTLPWDLWTTTSELVQPASSTAFNGFA QDTTAFAVQSNENVTETLTEAEEAPLGELKVEET | 435 |
| hAmph | PEVTPAGSAGVTHSPMSQTLPWDLWTTTSTDLVQPASGGSFNGFTQPQDTSLFTMQTQDNM AETEQALPTEPQAEEP | 440 |
| Rat Amph1 | PDVTPAGSAAATHSPMSQTLPWDLWTTTSTDLVQPASGGSFNDFTQPQDTSLFTMQTDQNM AETEQALPTEPQAEEP | 436 |
| Rat Amph2 | PVASPVKAP TPSGQSIPWDLW | 421 |

| | | |
|---|---|---|
| cAmph | PTAAVVEKEAILAEPDEPTEQAAESIEAGDKETTGIAEKE SEVVSAAGGAVAVEDSVVVAAG AGEGA VRTEQ | 507 |
| hAmph | LAAVTPAVGLDLGMDTRAEEP VEEAVIIPGADADAAVGTLVSAAEGAPGEEAEAEKATVPAGEGVSLEEAKIGTET | 516 |
| Rat Amph1 | PTTAAAPTAGLDLGLEM EEP KEEAAIPPGTDAGETVGT EGSTGEEAEAEKAAILPAGEGESPEGAKIDVES | 506 |
| Rat Amph2 | EPTESQAGVLPSGEPSSAEGSFAVAWPSQTAEPGPAQP | 481 |

| | | |
|---|---|---|
| cAmph | EAAAEGDKPQGEEKDVDVSQEKVSSIPSVVIEPASNNEGEGEEHHVIMNESKDAAAEMGTQGTDSETSQIGSEQKATEEI | 587 |
| hAmph | TEGAESAQPEAEELEATVPQEKV IPSVVIEPASNHEGEGENEITIGAEPKETTEDAAPPGPTSETPELATEQKPIQDP | 594 |
| Rat Amph1 | TELASSESPQAAELEAGAPQEKV IPSVVIEPASNHEGEHQETTTGTETREATEDVAPQGPAGEKQELATEPTP LDS | 583 |
| Rat Amph2 | AEASEVVGGTQEPGETAASEATSSSLPAVVVETFS | 494 |

| | | |
|---|---|---|
| cAmph | QTTPSQDQP ASAGDTASDMPPGFLFKVEVLHDFEAANSDELNLKRGDIVLVIPSETTADQEAGWLTGIKESEWL | 682 |
| hAmph | QPTPSAPAMGAADQLASAREASQELPPGFLYKVETLHDFEAANSDELTLQRGDVVLVVPSDSEADQDAGWLVGVKESDWL | 661 |
| Rat Amph1 | QAATPAPA GAVDASLSAGDAAQELPPGFLYKVETLHDFEAANSDELTLQRGDVVLVVPSDSEADQDAGWLVGVKESDWL | 662 |
| Rat Amph2 | ATVNGAVEGSTTTGRLDLPPGFMFKVQAQHDYTATDTDELQLKAGDVVLVTPFQNPEEQDEGWLMGVKESDWN | 567 |

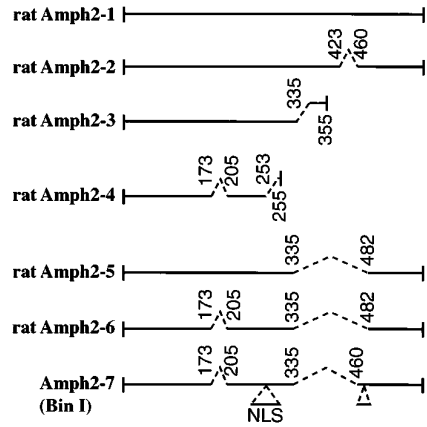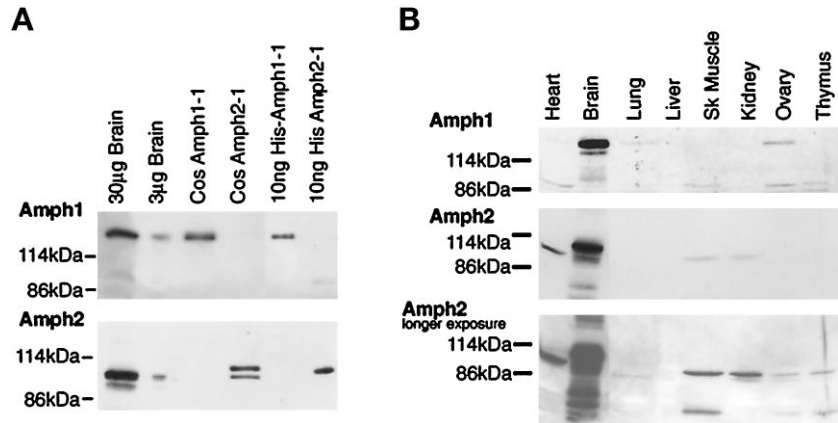| | | |
|---|---|---|
| cAmph | QYRDANSYKGLFPENFTRHLE | 682 |
| hAmph | QYRDLATYKGLFPENFTRRLD | 695 |
| Rat Amph1 | QYRDLATYKGLFPENFTRHLE | 683 |
| Rat Amph2 | QHKELEKCRGVFPENFTERVQ | 588 |

**B**



**C**



**Figure 1.** Primary structure of rat Amph2. (A) Sequence alignment showing homology of rat Amph2 to Amph1. Boxes show regions of amino acid identity in comparison to rat Amph1. The chick and human Amph sequences are shown for comparison. Amino acids conserved in among all SH3 domains are indicated with an asterisk. These sequences have been submitted to the GenBank database under accession numbers Y13380 (Amph2) and Y13381 (Amph1). (B) Overall comparison of Amph1 and Amph2. Amph is divided into four domains. Domain A is predicted to be α-helical and has a average pI of 9.0. Domain B is proline rich and acidic. Domain C is not conserved and acidic. Domain D is an SH3 module and acidic. (C) Amph2 splice variants. Comparison of Amph2 clones. Spliced introns are indicated by dotted lines. Note that Amph2–3 and Amph2–4 contain Amph2 sequence at their 3′ untranslated regions and, therefore, are unlikely to be cloning artifacts.

**Figure 2.** Characterization of Amph2 and its antiserum. (A) Amph2 is a 92-kDa protein present in the brain in the same molar ratio as Amph1. Total brain extract, extracts of COS cells transfected with either of the Amphs, and bacterially expressed protein were loaded on SDS-PAGE gels for comparison, followed by immunoblotting with each of the Amph antibodies. (B) Tissue distribution of Amph2 resembles that of Amph1. Brain extract (20 $\mu$g) and each of the other tissues (5 $\mu$g) were loaded on SDS-PAGE gels and immunoblotted with each antibody as indicated. A longer exposure of Amph2 reveals Amph2 reactivity in other tissues.

1992). We quantified the amounts of Amph present in brain, by calibration of antibody reactivity with standards of His-tagged Amphs. Amph2 is present in approximately the same abundance as Amph1, both constituting 0.1% of cell protein (Figure 2A). By comparison, dynamin is present at approximately 0.4% (our unpublished results).

To characterize the cellular distribution of Amph2, we immunoblotted various tissue fractions for Amph2 protein (Figure 2B). Amph2, like Amph1, is greatly enriched (at least 10-fold) in brain over peripheral tissues. Additionally, there appears to be a ubiquitous form of Amph2 at slightly lower molecular weight (probably Amph2–2). These results correlate with the presence of a ubiquitous Amph2 message on Northern blots that is smaller than the brain message and also the PCRs of the Amph2 cDNA being smaller from kidney and liver than brain.

Within the brain, both proteins are concentrated at nerve terminals (Figure 3). This can be visualized by immunocytochemistry where nerve terminals immunoreactive for Amph2 are widely distributed. The heaviest staining is observed in the cerebellum (Figure 3, A and B, bright areas), the pontine nucleus (Figure 3C) and in the hippocampus (particularly the CA1–CA3 pyramidal cell layer, our unpublished results). Within the cerebellum, nerve terminals containing Amph2 are found in all three layers. The large excitatory mossy fiber terminals of the granule cell layer appeared to be strongly reactive for this protein (Figure 3, B and F) and the Purkinje cell bodies are coated with many small round varicosities that stained positive for Amph2 (Figure 3B inset, and 3F). The molecular layer receives a dense plexus of Amph2-reactive terminals, which appear as punctate structures (Figure 3B). In the pontine nucleus, large numbers of neurons are heavily innervated by varicosities that are positive for Amph2 (Figure 3C). It is striking that Amph2 is highly enriched in a subset of terminals and weakly present in others. We suggest that Amph2 may be

highly associated with nerve terminals that have high levels of synaptic activity, because these terminals are packed with synaptic vesicles (Ohara and Lieberman, 1985). It was also noted that the staining of Amph2 is remarkably similar to that previously published for Amph1 (Lichte *et al.*, 1992).

Subcellular fractionation shows that both Amph1 and Amph2 are enriched in isolated nerve terminals (middle layer of sucrose gradient) to approximately the same extent as synaptic vesicle markers (Figure 3D). Within these terminals, the protein exists in two distinct pools, soluble and vesicle-associated (approximately 50% in each; Figure 3E). Immunoelectron microscopy was used to confirm the localization of Amph2 in nerve terminals at higher resolution, and it appears that, as has been reported previously for Amph1, the outer surface of synaptic vesicles (and also patches of the plasma membrane) is highly labeled for Amph2 (Figure 3, F and G). In addition, Amph2 behaves similarly to Amph1 in being highly resistant to extraction from membranes by high salt (up to 1 M KCl; our unpublished results). Thus, these data suggest that both Amph1 and Amph2, like dynamin, may be able to shuttle between membrane-bound and cytosolic pools.

### Investigation of Amph2-binding Partners

Because of the homology of the C-terminal domain of Amph2 to the SH3 domain of Amph1, the interaction of this domain with dynamin was tested. The C-terminal 94 amino acids were expressed and purified as a GST fusion protein, and the fusion protein was incubated with a crude extract of rat brain. An ~100-kDa doublet, which microsequencing revealed to be dynamin I, was specifically precipitated by this domain (Figure 4A). Thus, the sequence similarity of this region to Amph1 and other SH3 domains extends to a functional homology. The ligands of SH3 domains are proline-rich sequences, and so the Amph2 SH3 do-
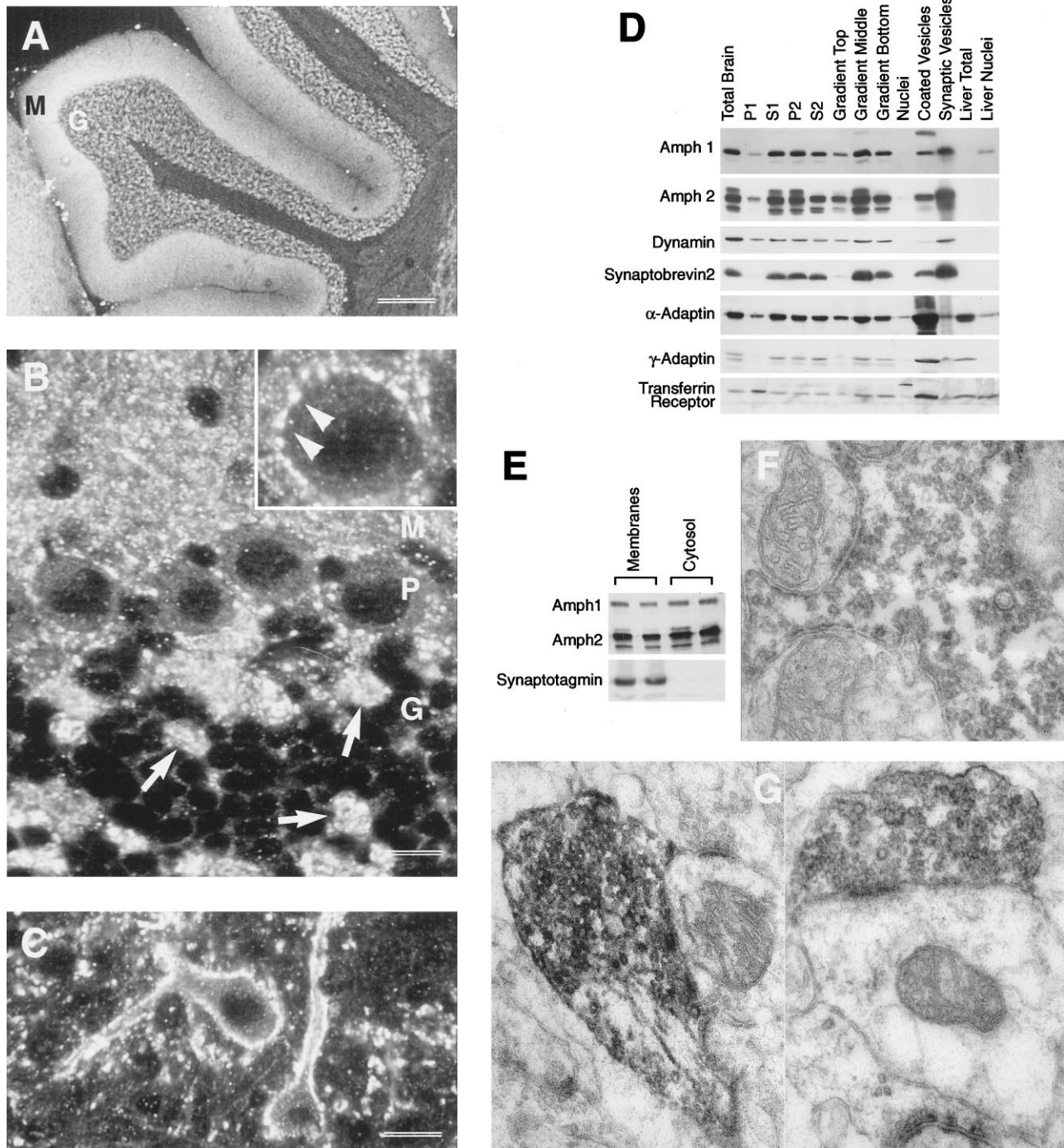
**Figure 3.** Subcellular distribution of Amph2 in rat brain. (A) By using Amph2 antiserum, the strongest staining for Amph2 is in the molecular (M) and granule cell (G) layers of the cerebellum. (B) At higher magnification, the presence of Amph in mossy fiber terminals of the granule cell layer (G) can be clearly seen (arrows). The Purkinje cell bodies (P) were surrounded by numerous small reactive terminals. This is more clearly seen in the inset (arrowheads). (C) Many cells in the pontine nucleus were densely innervated by fine Amph2 containing terminals. Bars: A, 300 $\mu$m; B, 14 $\mu$m; C, 9 $\mu$m. (D) Western blot analysis of subcellular fractions of rat brain. Subcellular fractionation was carried out according to MATERIALS AND METHODS. S1-P2 refer to successive pellets (P) or supernatants (S) of rat brain homogenized in 0.32 M buffered sucrose (see McMahon *et al.*, 1992). The P2 fraction contains crude synaptosomes and was used for Percoll gradient separation into three predominant layers, the middle layer of which is enriched in isolated nerve terminals. Five micrograms of protein were loaded in each lane. (E) Amph1 and Amph2 both exist as membrane-associated and cytoplasmic pools. Synaptosomes were hypotonically lysed, followed by pelleting at 150 000 × *g* for 30 min to obtain a crude membrane fraction and cytosol, cleared of all synaptic vesicles (as shown

main should interact with dynamin via its C-terminal polyproline region.

The C terminus of dynamin contains several overlapping clusters of proline-rich sequences, with potential for selectively binding different SH3 domain-containing proteins (Scaife *et al.*, 1994; Shpetner *et al.*, 1996). To examine whether Amph1 and Amph2 SH3 domains share the same polyproline target sequence, two peptides were synthesized, P1 (PAVPPARPG) and P2 (SPDPFGPPPQVPSRPNR). These were tested for their ability to compete with the SH3 domain–dynamin interaction of either Amph1 or Amph2 in brain extracts. Interestingly, although P2 (200 $\mu$M) efficiently blocks the Amph1–dynamin interaction, the binding of Amph2 SH3 domain is much less well inhibited (Figure 4B). Thus, either 1) the two Amph isoforms target different polyproline domains or 2) they bind to the same region but are differentially affected by P2 peptide inhibition due to different binding affinities. Recently, Okamoto *et al.* (1997) have identified the Amph1-binding sequence on dynamin to be GPPPQVPSRPNRA, and this has been further refined to the 6-residue sequence PSRPNR by Grabs *et al.* (1997). Our results therefore are consistent with these two studies.

### Amph2, Like Amph1, Is Phosphorylated in Synaptosomes by Protein Kinase C (PKC)

Given that Amph2 shares the ability of Amph1 to bind dynamin and possibly recruit it to coated pits, our results suggest that Amph2 may also have a role in synaptic vesicle endocytosis. Amph1 has been reported to exist as a phosphoprotein that is dephosphorylated upon stimulation (Bauerfeind *et al.*, 1995). To test whether the phosphorylation state of Amph2 is also affected by depolarization, we labeled synaptosomes with [$^{32}$P]orthophosphate, and immunoprecipitated for each of the Amphs. Amph2 immunoprecipitates contain a band at the correct size that is evidently labeled at resting potential and, upon the addition of 35 mM KCl to stimulate the synaptosomes, Amph2 is rapidly dephosphorylated by approximately 50% (Figure 5A). Compared with Amph1 and dynamin I, this dephosphorylation is more extensive. Indeed, the effect can be reversed by repolarizing the presynaptic membrane (return



**Figure 4.** Amph2 associates with dynamin in vitro. (A) The SH3 domain of Amph2, like Amph1, binds specifically and stoichiometrically to dynamin in brain extracts. GST fusion proteins, and GST as a control, were incubated with brain extract followed by analysis of bound proteins by SDS-PAGE and Coomassie staining. Note the presence of a fainter ~145-kDa band (probably synaptojanin). (B) The P2 peptide differentially affects dynamin binding to Amph1 and Amph2. GST-tagged SH3 domains were incubated as in A but in the presence or absence of each of the indicated peptides (at a concentration of 200 $\mu$M). Bound dynamin was visualized by Coomassie blue staining.

to 5 mM KCl), bringing both Amphs back to their original phosphorylation state (Figure 5B). This suggests that both Amphs can be reversibly dephosphorylated upon stimulation of exocytosis, further implicating the function of Amph2 in synaptic vesicle recycling. Thus, all three proteins might be dephosphorylated as a complex. A similar cycling of the dynamin I phosphorylation state has been observed (Robinson *et al.*, 1994).

The kinase for Amph has not been identified to date, and to address whether it may also be PKC, we treated synaptosomes with the PKC activator phorbol 12-myristate 13-acetate (PMA), or the specific PKC inhibitor Ro31–8220, during phosphate labeling. Figure 5C shows that Amph1, Amph2, and dynamin are hyperphosphorylated in the presence of PMA, and this labeling is reduced with the PKC inhibitor, implying that all three proteins share the same a common kinase.

---

**Figure 3 (cont).** by synaptotagmin control). Each fraction was loaded in duplicate, at 10 $\mu$g of protein per lane. (F and G) Electron micrographs showing the ultrastructural localization of Amph2 in the rat cerebellum. The large mossy fiber terminals in the granule cell layer were found to be heavily stained with Amph2 reaction product (F), as were climbing fiber terminals in the molecular/Purkinje cell layer (G). Within these structures, Amph2 staining was heavily concentrated on the outer layer of synaptic vesicles.
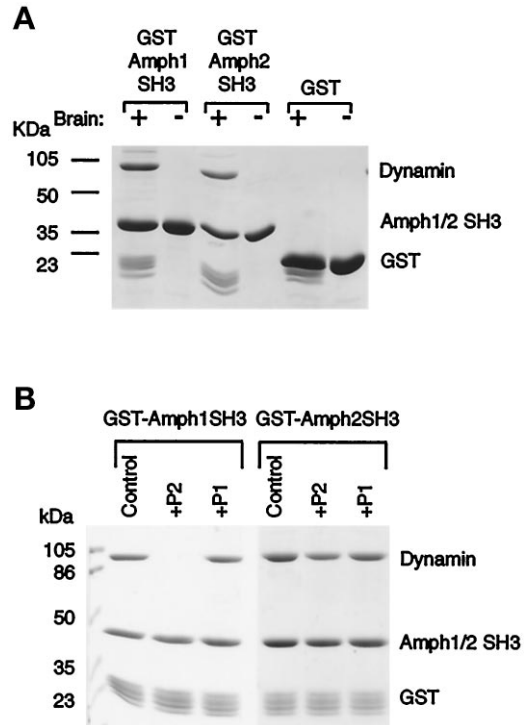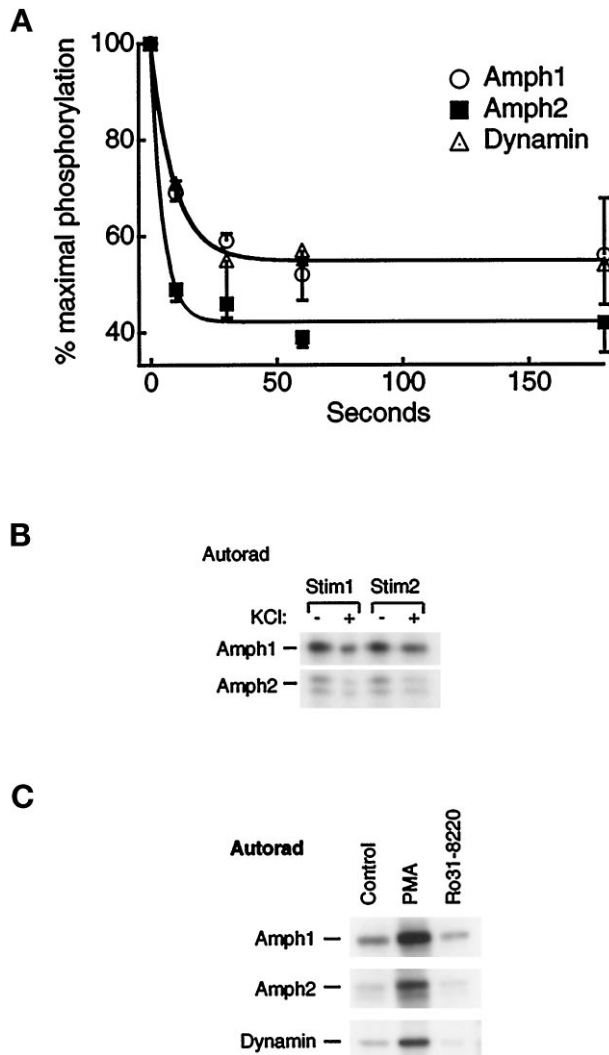
**A**



**B**



**C**



**Figure 5.** Amph phosphorylation and dephosphorylation. (A) Time course of Amph2 dephosphorylation is more rapid and extensive than Amph1 or DynI. Seconds refer to the time after addition of KCl. Data are averaged from four separate experiments (means ± SEM). (B) Repetitive depolarization/repolarization of synaptosomes induces cyclical changes in the phosphorylation state of the Amphs. After the first stimulation (Stim1), synaptosomes were pelleted for 5 s at 13,000 × *g* and resuspended in repolarization buffer (HBM containing 4.5 mM KCl), allowed to equilibrate for 1 min at 37°C, before addition of KCl back to 35 mM (Stim2). Dynamin, Amph1, and Amph2 were immunoprecipitated with their respective antiserum. (C) Effect of PKC activator (PMA) and inhibitor (Ro31–8220) on the phosphorylation state of Amph1 and Amph2. Synaptosomes were labeled as described in A and 10 μM of either PMA or Ro31–8220 were added just before harvesting.

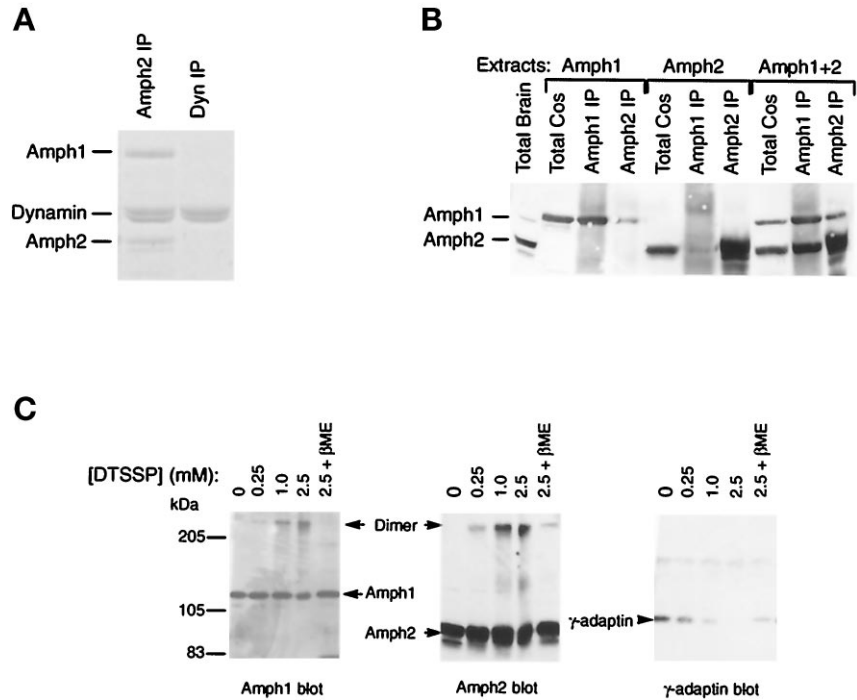### Amph2 Forms Heterodimers with Amph1

The subcellular colocalization of Amph1 and 2 and their parallel dephosphorylation shown in Figure 5A suggest that Amph1 forms a complex in the brain with Amph2. To test this directly, Amph2 immunoprecipitates were Coomassie-stained, revealing that Amph1

and Amph2 are coprecipitated and, moreover, that the two proteins are in an equimolar ratio (Figure 6A). Densitometry from 10 immunoprecipitations gave a mean Amph1 to Amph2 ratio of 1.04 ± 0.09. Although significant, the coprecipitation of the two isoforms could merely be due to cross-reactivity of the antibody to the other isoform. This was tested by immunoprecipitations from COS cells transiently transfected with Amph1 or Amph2 or the two together (Figure 6B). The Amph1 and Amph2 antisera cross-react very weakly at the level of immunoprecipitations; i.e., the Amph1 antiserum precipitates very little Amph2, and vice versa. In cells coexpressing the two isoforms, however, either antibody coprecipitates both Amph1 and Amph2 (Figure 6B). Amph1 and Amph2 do not interact to form a stable complex in vitro upon the addition of separately expressed Amphs, indicating that two proteins need to be coexpressed in vivo for association to occur.

These data strongly suggest Amph1 and Amph2 form a complex in vivo. To determine the size of this heterooligomer, cross-linking was used. 3,3′-Dithiobis(sulfosuccinimidylpropionate) (DTSSP), a homobifunctional cross-linker that is cleaved by 2-mercaptoethanol, was incubated with rat brain cytosol. A band at 220–250 kDa that is reactive to both anti-Amph1 and anti-Amph2 antibodies, and therefore containing both isoforms, is present only in the sample containing cross-linker, and disappears upon boiling in 2-mercaptoethanol (Figure 6C). This molecular weight is equivalent to the sum total of the apparent masses of Amph1 (125 kDa) and Amph2 (92 kDa). As a control antibody, anti-γ-adaptin did not react to the same band. The same adduct was found after incubation of synaptosomes with a membrane-permeable cross-linker. It is perhaps surprising that, although dynamin was found in immunoprecipitates of the heterodimer, it was never found cross-linked with the complex (our unpublished results). This probably reflects the fact that the area for contact between dynamin's polyproline site and the SH3 domains consists of only a few residues, none of which are lysines (McMahon and Owen, unpublished data) upon which the cross-linkers depend.

To further confirm the existence of a stoichiometric homogenous heterodimer in brain extracts, a combination of gel filtration and sucrose density gradient centrifugation was used. Immunoblotting revealed perfect comigration of Amph1 and Amph2 into a single peak, consistent with a heterodimer (our unpublished results). The molecular weight of the complex could not be estimated accurately because of its anomalous migration in both fractionation procedures due to a highly extended conformation of the Amph complex (McMahon and Owen, unpublished data). These data and the fact that the Amph2 immunoprecipitate in Figure 6A precipitates the two isoforms in a 1:1 ratio

**Figure 6.** Amph1 and Amph2 form heterodimers in vivo. (A) Immunoprecipitation of Amph1 and Amph2 from brain as an equimolar complex. Rat brain extract in buffer A was immunoprecipitated with antiserum to either Amph2 or, as a control, dynamin. Bound proteins were analyzed by Coomassie blue staining. Note the presence of dynamin in both immunoprecipitates (see Figure 8A). (B) Immunoprecipitation of the two isoforms as a complex in COS cells. COS cells were transiently transfected with Amph1, Amph2, or the two together. Extracts of each were separately immunoprecipitated with antibodies against Amph1 or Amph2 and processed for Western blotting. Total proteins were also loaded to show the starting material. (Due to the strength of the Amph2 antibody, total brain (lane 1) appears to have a much higher level of Amph2 compared with Amph1, but as we have shown in Figure 2A, they are present in a 1:1 ratio.) (C) Cross-linking with DTSSP suggest the Amph1–Amph2 oligomer is a heterodimer. Rat brain cytosol (10 mg/ml) was incubated with different concentrations of DTSSP and separated by SDS-PAGE on 7% gels before blotting with the antibodies indicated.



suggest that the heterodimer is the predominant form of Amph in the brain.

### The Heterodimer Binds to Multiple Dynamin Molecules and Accelerates Dynamin's GTPase Activity

The SH3 domains of either Amph1 or 2 both bind dynamin in a 1:1 molar ratio (Figure 4A). However, Figure 6A shows that the amount of dynamin bound to the heterodimer is approximately 2:1 (mean ratio of 1.8, from five experiments). Thus, both Amph SH3 domains in the dimer seem to be accessible to bind separate dynamin molecules. We tested whether this is the case by immunoprecipitating the heterodimer under conditions identical to those for the experiment shown in Figure 4B. In the presence of 200 $\mu$M peptide P2, which blocks the Amph1SH3–dynamin interaction, but not the Amph2SH3–dynamin interaction (see Figure 4B), the amount of bound dynamin is reduced by only ~60% (Figure 7A). As further evidence that both SH3 domains are accessible, the bacterially expressed heterodimer can bind twice as much dynamin as an equivalent molar amount of Amph1 or Amph2 (our unpublished results). As an additional control, 1 M NaCl completely eluted dynamin from the dimer (Figure 7A), which shows that the dimerization of Amph1 to Amph2 is a very stable interaction and, moreover, does not depend on dynamin.

Association of the heterodimer with multiple dynamins in the Amph2 immunoprecipitate raised the possibility that, in recruiting dynamin, Amph1+2 may act as an initiation points for dynamin oligomerization. Such assembly of dynamin (possibly into helical rings) has been proposed to cause an increased
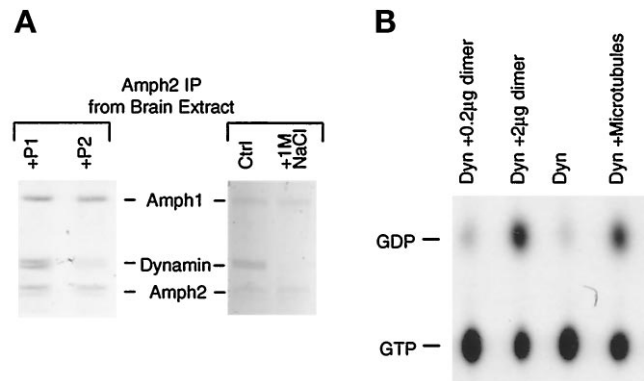


**Figure 7.** The heterodimer binds tightly to dynamin and increases its GTPase. (A) Effect of peptides and high salt treatment on dynamin binding to the heterodimer. Amph2 immunoprecipitations of brain extract were done in buffer A containing 200 $\mu$M peptide P1 or P2 (left) or in different salt concentrations (right; Ctrl, low salt [buffer A]; 1M NaCl, high salt wash) and separated by SDS-PAGE on 7% gels for Coomassie staining. (B) The heterodimer activates dynamin's GTPase in vitro. Purified dynamin was incubated with [$\alpha$-$^{32}$P]GTP in the presence of different effectors. The heterodimer (0.2 $\mu$g in lane 1 and 2.0 $\mu$g in lane 2) was purified from brain cytosol by Amph2 immunoprecipitation. All reactions were brought to the same dynamin concentration (0.5 $\mu$g in 50 $\mu$l). Taxol-polymerized microtubules were included as a positive control.
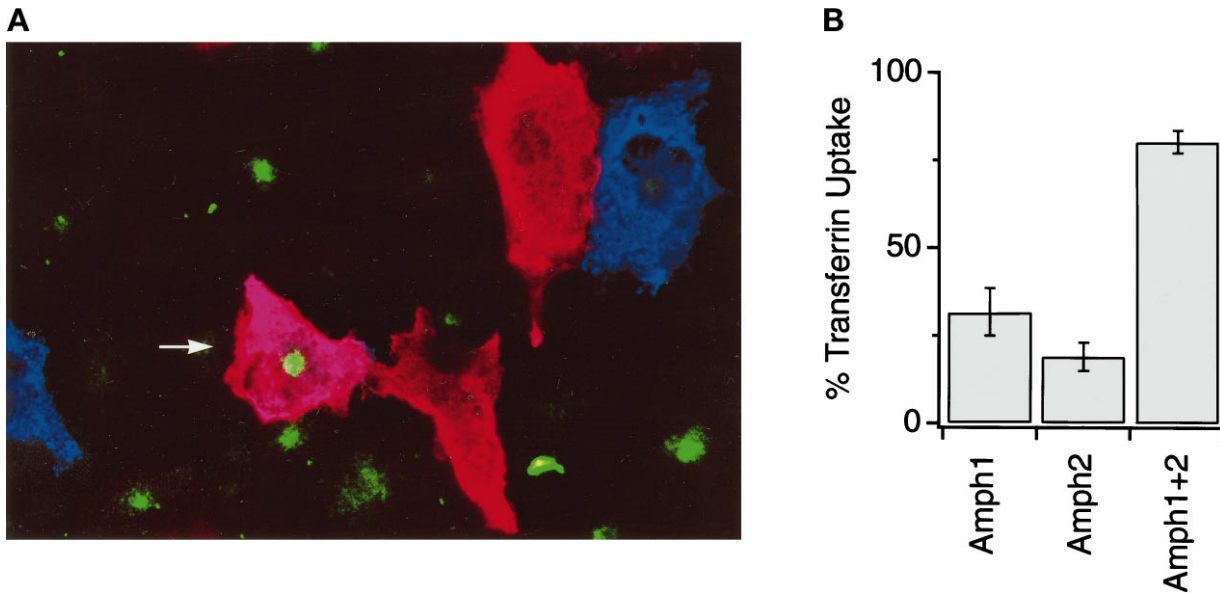
**A**

**B**



**Figure 8.** Support for heterodimer formation and function in COS cells. (A) Immunofluorescence micrograph showing a blockade of transferrin uptake (green perinuclear staining) in cells overexpressing Amph1 (stained red) or Myc-Amph2 (stained blue). The mauve cell marked with an arrow is cotransfected with both constructs (and therefore overexpressing both isoforms) and takes up transferrin normally. The transferrin uptake assay was done according to Wigge *et al.* (1997). (B) Quantitation of the effect. Sixty cells (20 from each category) were measured for transferrin uptake and the mean value was expressed as a percentage of normal transferrin uptake (i.e., that of untransfected cells).

GTPase activity of dynamin (Warnock *et al.*, 1996), and this could be necessary in vivo, because GTP hydrolysis is postulated to drive fission of the collared vesicle. We therefore tested the effect of the heterodimer on dynamin's GTPase activity. Immunoprecipitation with the Amph2 antibody was used to purify the heterodimer from brain cytosol, and when added to the GTPase reaction, the heterodimer greatly increased the conversion of GTP to GDP (Figure 7B). This is similar to the effect of microtubules, which was included as a positive control. In contrast, individual SH3 domains of either Amph1 or Amph2 failed to activate dynamin's GTPase to a significant extent (our unpublished results). Thus, these results suggest that the heterodimer may have a special function in recruiting multiple dynamins (and therefore acting as a template for oligomerization) or in regulating dynamin's GTPase cycle.

### Transferrin Uptake in COS Cells Is Blocked by Overexpression of Amph1 or Amph2 but Is Rescued by Their Coexpression

We have previously shown that the SH3 domain of Amph 1 exerts a dominant negative effect on receptor-mediated endocytosis in COS cells, likely by preventing dynamin recruitment to clathrin-coated pits (Wigge *et al.*, 1997). We used the same transferrin uptake assay to answer the question of whether full-

length Amph1 could exert the same effect. Amph1 caused a potent block (red blood cells, Figure 8A) as scored by the absence of transferrin uptake (perinuclear green staining). The inhibition is observed in the majority of cells as quantitated in the bar graph (Figure 8B). Myc-tagged Amph2 also caused a similar inhibition of transferrin uptake (blue cell in Figure 8A). This provided us with a useful tool to test the importance of the heterodimer in vivo. We cotransfected the two plasmids and show that cells coexpressing both isoforms (pink cell) are rescued in transferrin uptake (see Figure 8B). We interpret these results to mean that either Amph1 or Amph2 overexpression alone leads to sequestration of endogenous dynamin into inactive complexes, but when the two proteins are expressed together, forming a heterodimer, endocytosis can resume. It appears that only the heterodimer can form a functional complex with dynamin and so participate in the endocytic cycle.

## DISCUSSION

In this article we have investigated the properties of Amph2, in the possibility that it might represent an isoform functionally distinct from Amph1, perhaps participating in endocytic events other than synaptic vesicle recycling at the plasma membrane. Instead, we find that the subcellular distribution and phosphory-

lation and membrane association properties of both Amphs closely parallel each other. This suggests that the two proteins act in concert, and indeed, coexpression of the two isoforms in COS cells or in bacteria is sufficient to generate a stable equimolar complex. Cross-linking indicates that this complex exists in vivo as a 220- to 250-kDa heterodimer. Furthermore, the dimer appears to be the predominant form of Amph in the brain, where it can be coimmunoprecipitated with multiple molecules of dynamin I and, therefore, is the likely form of Amph that drives the recruitment of dynamin to sites of clathrin-mediated endocytosis. It is interesting that Amph1, Amph2, and dynamin I are rapidly dephosphorylated in parallel upon nerve-terminal stimulation. On repolarization they are all rephosphorylated by the same kinase, PKC, further supporting the idea that they might function as a complex.

Two Amph homologues, *rvs161* and *rvs167*, have been identified in *Saccharomyces cerevisiae* (David *et al.*, 1994; Munn *et al.*, 1995; Sivadon *et al.*, 1995). Knocking out either of the *rvs* genes leads to the full endocytosis-defective phenotype characteristic of the double mutant. Furthermore, both mutant strains are suppressed by the same set of SUR genes (Desfarges *et al.*, 1993). This has led to the hypothesis that the two proteins function as a complex, possibly a heterodimer, at least in yeast (Bauer *et al.*, 1993). Although sharing only weak sequence homology to the yeast proteins, Amph1 and Amph2 also form heterodimers, and in this respect at least, the heterodimer appears to have been conserved throughout evolution.

Whether or not the heterodimer has been conserved in function is less clear. The in vivo transferrin uptake assay clearly shows that, although overexpression of either Amph1 or Amph2 alone blocks endocytosis in COS cells, formation of the Amph1–Amph2 heterodimer rescues this defect. This suggests that the heterodimer has a crucial function not fulfilled by the separate Amphs. What is this function? Although Amph1 and Amph2 separately bind dynamin in vitro, the brain heterodimer can interact with multiple dynamin molecules simultaneously and, therefore, bind more on a molar basis than either Amph1 or Amph2. This would imply that both SH3 domains in the heterodimer are accessible to interact with separate dynamin molecules. In synaptic vesicle endocytosis, Amph heterodimers localized to the plasma membrane (probably via an interaction with the AP-2 adaptor complex; Wang *et al.*, 1995; David *et al.*, 1996) would allow for efficient recruitment of multiple dynamin molecules to the coated pit. By generating a high local concentration of dynamin molecules in this way, Amph could potentially act as a template for the nucleation of dynamin oligomers, aiding the assembly of dynamin into rings at the neck of the constricted coated pit (Figure 9). Although this hypothesis remains to be tested, our experiments showing that the
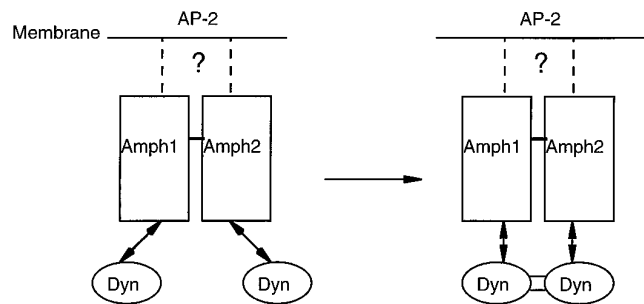


**Figure 9.** Hypothetical model for the action of the Amph heterodimer in dynamin recruitment. The SH3 domains of both isoforms are accessible in the dimer to interact with separate dynamin molecules, which are brought into close proximity, catalyzing the formation of intermolecular links leading to oligomerization. The heterodimer is likely to be membrane localized through its interaction with AP-2 adaptor complexes (the question mark in the diagram). Amph1 and Amph2 probably dimerize through coiled-coil interactions between their N-terminal α-helical domains (a region weakly conserved with the Rvs proteins). Dissociation of the complex could be brought about by dynamin's GTPase activity, breaking up the oligomer and returning the separate components to the cytosol.

heterodimer (but not either isolated Amph SH3 domain) accelerates dynamin's GTPase activity in vitro lends support to this model. GTP hydrolysis by dynamin is thought to be a necessary prerequisite for the concerted conformational change in the oligomer that pinches off the vesicle (De Camilli *et al.*, 1995). If Amph has an important role in this cycle, it is likely that the GTPase activation is tightly controlled; GTP hydrolysis in the cytosol would be premature. To be physiological, Amph should only activate GTP hydrolysis on dynamin when it is assembled at the collar of the coated pit. In vivo, therefore, it is important not to rule out other factors that may come into play as well as Amph.

Why are there so many splice variants of Amph2? We have identified six different alternatively spliced forms; at least some of these are present in peripheral tissues and, therefore, could have more generalized roles. It is interesting that both Amph2–3 and Amph2–4 lack the C-terminal SH3 domain and in this respect resemble the domain structure of the yeast homologue *rvs161*. The yeast heterodimer, lacking the two SH3 domains characteristic of the rat brain heterodimer we have characterized, would probably have a different function. Such a dimer would not be able to recruit multiple dynamin molecules. It is possible, then, that the brain heterodimer is a feature of the specialized pathway of synaptic vesicle uptake and reflects the need for rapid or efficient dynamin recruitment to endocytosing zones of nerve terminals. Yeast, which does not require such rapid membrane uptake, could cope with just one SH3 domain. However, the yeast dynamin homologue interacting with

the Rvs167 protein remains to be identified, and so endocytosis in this organism could, in theory at least, act by a different mechanism entirely.

Particularly intriguing is the possibility that a collection of Amph heterodimers could exist, each with slightly different binding specificities. In this context, we have preliminary data suggesting that Amph2–6, and possibly other splice variants, can heterodimerize with Amph1. The transcription factors Fos and Jun exist in different combinations of dimeric forms, each of which display different DNA-binding specificities. It is possible that a repertoire of different Amph heterodimers could greatly expand the potential for regulation of clathrin-mediated uptake processes.

Although much evidence indicates that the Amph family takes part in endocytosis at the plasma membrane, a second distinct role for one of the Amph2 splice variants, Amph2–7, has been suggested. This isoform has been recently isolated as the nuclear Myc-interacting protein BIN1 (Sakamuro *et al.*, 1996). Loss of BIN1 mRNA was frequently observed in tumor cell lines, and BIN1 prevented tumorigenesis by Ras in a cooperativity assay. Thus, these data led Sakamuro *et al.* (1996) to suggest that BIN1 is a tumor suppressor. Although we found a partial clone encoding a nuclear localization signal, this was not predominant in the cDNA library. We have no other data to support a different function for Amph2, but it is possible that this gene product, depending on how it is spliced and, therefore, to which compartment it is targeted, has the capacity to play two diverse roles in the cell. Proenkephalin, normally a cytoplasmic protein that is destined to be secreted, has also been found to have a possibly distinct function in the nucleus (Bottger and Spruce, 1995). These authors hypothesized that the two diverse roles of the protein may reflect a molecular economy in the process of evolution, such that "gene sharing" has been adopted.

The heterodimer appears to be the main form of Amph in the brain, and a combination of in vitro and in vivo data suggest it may have an important widespread role in clathrin-mediated endocytosis not fulfilled by either isoform alone.

*Note Added in Proof.* After submission of this manuscript, three groups independently reported the cloning and characterization of Amph2 (Butler *et al.*, 1997; Leprince *et al.*, 1997; Ramjaun *et al.*, 1997).

## ACKNOWLEDGMENTS

## REFERENCES

Bauer, F., Urdaci, M., Aigle, M., and Crouzet, M. (1993). Alteration of a yeast SH3 protein leads to conditional viability with defects in cytoskeletal and budding patterns. Mol. Cell Biol. *13*, 5070–5084.

Bauerfeind, R., David, C., and De Camilli, P. (1995). Amphiphysin, a nerve-terminal protein with a putative function in synaptic vesicle endocytosis, is dephosphorylated upon stimulation of neurotransmitter release. Mol. Biol. Cell *6* (suppl), 405a.

Bottger, A., and Spruce, B.A. (1995). Proenkephalin is a nuclear protein responsive to growth arrest and differentiation signals. J. Cell Biol. *130*, 1251–1262.

Butler, M.H., David, C., Ochoa, G.C., Freyberg, Z., Daniell, L., Grabs, D., Cremona, O., and De Camilli, P. (1997). Amphiphysin II (SH3P9; BIN1), a member of the amphiphysin/Rvs family, is concentrated in the cortical cytomatrix of axon initial segments and nodes of ranvier in brain and around T tubules in skeletal muscle. J. Cell Biol. *137*, 1355–1367.

Clark, S.G., Stern, M.J., and Horvitz, H.R. (1992). *C. elegans* cell-signalling gene *sem-5* encodes a protein with SH2 and SH3 domains. Nature *356*, 340–344.

Crouzet, M., Urdaci, M., Dulau, L., and Aigle, M. (1991). Yeast mutant affected for viability upon nutrient starvation: characterisation and cloning of the *rvs161* gene. Yeast *7*, 727–743.

Damke, H., Baba, T., Warnock, D.E., and Schmid, S.L. (1994). Induction of mutant dynamin specifically blocks endocytic coated vesicle formation. J. Cell Biol. *127*, 915–934.

David, C., McPherson, P.S., Mundigl, O., and De Camilli, P. (1996). A role of amphiphysin in synaptic vesicle endocytosis suggested by its binding to dynamin in nerve terminals. Proc. Natl. Acad. Sci. USA *93*, 331–335.

David, C., Solimena, M., and De Camilli, P. (1994). Autoimmunity in stiff-man syndrome with breast cancer is targeted to the C-terminal region of human amphiphysin, a protein similar to the yeast proteins, Rvs167 and Rvs161. FEBS Lett. *351*, 73–79.

De Camilli, P., Takei, K., and McPherson, P.S. (1995). The function of dynamin in endocytosis. Curr. Opin. Neurobiol. *5*, 559–565.

Desfarges, L., Durrens, P., Juguelin, H., Cassagne, C., Bonneu, M., and Aigle, M. (1993). Yeast mutants affected in viability upon starvation have a modified phospholipid composition. Yeast *9*, 267–277.

Fykse, E.M., Takei, K., Walch-Solimena, C., Geppert, M., Jahn, R., De Camilli, P., and Sudhof, T.C. (1993). Relative properties and localisations of synaptic vesicle protein isoforms: the case of the synaptophysins. J. Neurosci. *13*, 4997–5007.

Grabs, D., Slepnev, V.I., Songyang, Z., David, C., Lynch, M., Cantley, L.C., and De Camilli, P. (1997). The SH3 domain of amphiphysin binds the proline-rich domain of dynamin at a single site that defines a new SH3 binding consensus sequence. J. Biol. Chem. *272*, 13419–13425.

Herskovits, J.S., Burgess, C.C., Obar, R.A., and Vallee, R.B. (1993). Effects of mutant rat dynamin on endocytosis. J. Cell Biol. *122*, 565–578.

Hinshaw, J.E., and Schmid, S.L. (1995). Dynamin self-assembles into rings suggesting a mechanism for coated vesicle budding. Nature *374*, 190–192.

Leprince, C., Romero, F., Cussac, D., Vayssiere, B., Berger, R., Tavitian, A., and Camonis, J.H. (1997). A new member of the amphiphysin family connecting endocytosis and signal transduction pathways. J. Biol. Chem. *272*, 15101–15105.

Lichte, B., Veh, R.W., Meyer, H.E., and Killimann, M.W. (1992). Amphiphysin, a novel protein associated with synaptic vesicles. EMBO J. *11*, 2521–2530.

McMahon, H.T., Foran, P., Dolly, J.O., Verhage, M., Wiegant, V.M., and Nicholls, D.G. (1992). Tetanus toxin and botulinum toxins type A and B inhibit glutamate, gamma-aminobutyric acid, aspartate, and met-enkephalin release from synaptosomes. Clues to the locus of action. J. Biol. Chem. *267*, 21338–21343.

McMahon, H.T., and Nicholls, D.G. (1991). Transmitter glutamate release from isolated nerve terminals: evidence for biphasic release and triggering by localised $Ca^{2+}$. J. Neurochem. *56*, 86–94.

McMahon, H.T. and Südhof, T.L. (1995) Synaptic core complex of synaptobrevin, syntaxin, and SNAP25 forms high affinity $\alpha$-SNAP binding site. J. Biol. Chem. *270*, 2213–2217.

Munn, A.L., Stevenson, B.J., Geli, M.I., and Riezman, H. (1995). *end5*, *end6* and *end7*: mutations that cause actin delocalization and block the internalization step of endocytosis in *Saccharomyces cerevisiae*. Mol. Biol. Cell *6*, 1721–1742.

Ohara, P.T., and Lieberman, A.R. (1985). The thalamic reticular nucleus of the adult rat: experimental anatomical studies. J. Neurocytol. *14*, 365–411.

Okamoto, P.M., Herskovits, J.S., and Vallee, R.B. (1997). Role of the basic, proline-rich region of dynamin in src homology 3 domain binding and endocytosis. J. Biol. Chem. *272*, 11629–11635.

Poodry, C.A., and Edgar, L. (1979). Reversible alterations in the neuromuscular junctions of *Drosophila melanogaster* bearing a temperature-sensitive mutation, *shibire*. J. Cell Biol. *81*, 520–527.

Ramjaun, A.R., Micheva, K.D., Bouchelet, I., and McPherson, P.S. (1997). Identification and characterization of a nerve terminal-enriched amphiphysin isoform. J. Biol. Chem. *272*, 16700–16706.

Robinson, P.J., Liu, J.-P., Powell, K.A., Fykse, E.M., and Sudhof, T.C. (1994). Dynamin GTPase regulated by protein kinase C phosphorylation in nerve terminals. Nature *365*, 163–166.

Sakamuro, D., Elliott, K.J., Wechsler-Reya, R., and Prendergast, G.C. (1996). BIN1 is a novel MYC-interacting protein with features of a tumour suppressor. Nat. Genet. *14*, 69–77.

Scaife, R., Gout, I., Waterfield, M.D., and Margolis, R.L. (1994). Growth factor-induced binding of dynamin to signal transduction proteins involves sorting to distinct and separate proline-rich dynamin sequences. EMBO J. *13*, 2574–2582.

Shpetner, H.S., Herskovits, J.S., and Vallee, R.B. (1996). A binding site for SH3 domains targets dynamin to coated pits. J. Biol. Chem. *271*, 13–16.

Shupliakov, O., Low, P., Grabs, D., Gad, H., Chen, H., David, C., Takei, K., De Camilli, P., and Brodin, L. (1997). Synaptic vesicle endocytosis impaired by disruption of dynamin-SH3 domain interactions. Science *276*, 259–263.

Sivadon, P., Bauer, F., Aigle, M., and Crouzet, M. (1995). Actin cytoskeleton and budding pattern are altered in the yeast *rvs161* mutant: the Rvs161 protein shares common domains with the brain protein amphiphysin. Mol. Gen. Genet. *246*, 485–495.

Takei, K., McPherson, P.S., Schmid, S.L., and De Camilli, P. (1995). Tubular membrane invaginations coated by dynamin rings are induced by GTP$\gamma$S in nerve terminals. Nature *374*, 186–190.

Vallee, R.B., and Okamoto, P.M. (1995). The regulation of endocytosis: identifying dynamin's binding partners. Trends Cell Biol. *5*, 43–48.

van der Bliek, A.M., Redelmeier, T.E., Damke, H., Tisdale, E.J., Meyerowitz, E.M., and Schmid, S.L. (1993). Mutations in human dynamin block an intermediate stage in coated vesicle formation. J. Cell Biol. *122*, 553–563.

Wang, L.-H., Sudhof, T.C., and Anderson, R.G.W. (1995). The appendage domain of $\alpha$-adaptin is a high affinity binding site for dynamin. J. Biol. Chem. *270*, 10079–10083.

Warnock, D.E., Hinshaw, J.E., and Schmid, S.L. (1996). Dynamin self-assembly stimulates its GTPase activity. J. Biol. Chem. *271*, 22310–22314.

Wigge, P., Vallis, Y., and McMahon, H.T. (1997). Inhibition of receptor-mediated endocytosis by the amphiphysin SH3 domain. Curr. Biol. *7*, 554–560.